Inorganic Chemistry

Article

pubs.acs.org/IC

Intercalation of Azamacrocyclic Crown Ether into Layered Rare-Earth Hydroxide (LRH): Secondary Host–Guest Reaction and Efficient Heavy Metal Removal

Weili Li, Qingyang Gu, Feifei Su, Yahong Sun, Genban Sun, Shulan Ma,* and Xiaojing Yang

Beijing Key Laboratory of Energy Conversion and Storage Materials, College of Chemistry, Beijing Normal University, Beijing 100875, P. R. China

Supporting Information

ABSTRACT: A carboxyethyl substituted azacrown ether (CSAE) derivative was intercalated as a second host into a parent host of layered gadolinium hydroxides (LGdH) by an anion-exchange reaction. The influence of intercalation temperature and starting material ratios of CSAE/LRH on the structures and compositions of CSAE-LRH nanocomposites were investigated. Higher temperature and larger initial CSAE-LGdH weight ratios favor of higher degree of ion exchange at a certain range, while lower temperature gives good morphology for the composites. The adsorptive properties for transition and heavy metal ions were studied using the 20 °C-reacted composite, which showed higher adsorptivity toward transition and heavy metal ions, accompanied by the introduction of nitrate anions. The adsorptive capacity for transition metal ions was in the sequence of Cu^{2+} > Zn^{2+}~Ni^{2+}~Co^{2+} with a high selectivity to Cu^{2+}. For the heavy metal ions Ag^{+}, Hg^{2+}, Pb^{2+}, and Cd^{2+}, the composite showed markedly high selectivity for Ag^{+} and Hg^{2+}. When putting Cu^{2+}, Ag^{+}, Hg^{2+}, Pb^{2+}, and Cd^{2+} together, Ag^{+} and Hg^{2+} still have higher adsorptive selectivity over Pb^{2+} and Cd^{2+}, and Cu^{2+} has also relatively high selectivity but not as high as Ag^{+} and Hg^{2+}. The nanocomposites with a second host in the interlayer are one promising kind of material because of the synergy of the steric effect of the parent host (LRH layer) and the particular characteristics of the secondary host (interlayer crown ether anions).

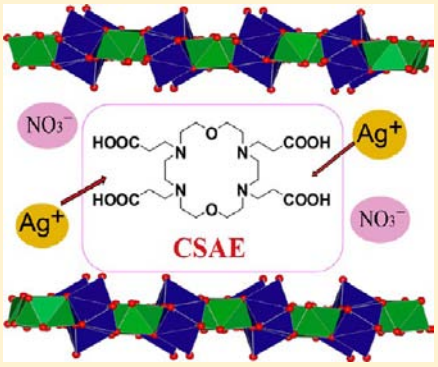

INTRODUCTION

In recent years, organic/inorganic composite materials, which combine organic compounds and inorganic ones through synergistic effect of each component in the nanometer range, have become the research hotspot nowadays.[1] Layered inorganic compounds have been extensively studied in the fields of materials chemistry, owing to their wide range of applications in rechargeable batteries, pollutant trapping, heterogeneous catalysis, drug delivery, microelectronics, and so forth.[2] Layered rare-earth hydroxides (LRHs) are one new class of anionic layered compounds that have attracted considerable attention since their emergence in 2006.[3] LRHs are composed of cationic lanthanide hydroxide layers and interlayer anions, with a general chemical formula of $RE_2(OH)_{6-m}(A^{x-})_{m/x}{\cdot}nH_2O$ (RE: rare-earth ions; A: guest anions). LRHs have facile anion exchange ability similar to classical layered double hydroxides (LDHs), but sometimes are much superior with respect to the latter. In LRHs, the two types of Ln coordination motifs of 8-fold dodecahedron polyhedron and 9-fold monocapped square antiprism, along with the coordinated water molecules, mean a much different layer structure. Besides, the lanthanide ions in LRHs have unique 4f electron configuration energy levels, which may bring new features that impel them to be used in many areas such as medical,[4] optical,[5] catalysis,[3,6] and in other materials. The combination of LRH host layers with organic guests can bring about novel properties because of the synergistic effect of the containing components; however, the investigations about LRHs mainly have focused on the anion-exchange, calcination behaviors, or luminescence property involving inorganic anions in the interlayer.[7] The studies on LRH intercalation with organic guests are much scarcer except for rare examples[7a,8] especially those reported by our group involving the luminescence property for Eu^{3+} containing LRH intercalates with benzenepolycarboxylic organic compounds.[9]

Macrocyclic compounds, including calixarenes, cyclodextrins, crown ethers, are one important kind of organic molecules having applications in structural assembly[10] and molecule/ion recognition.[11] The macrocyclic compounds can be inserted into layered inorganic compounds to form new solids, in which the introduced macrocycles may serve as secondary hosts to recognize guest species, and the new solid phases can be used in the area of adsorption separation and heterogeneous catalysis. Most of the related studies involved intercalation of the macrocycles, mainly cyclodextrins, into inorganic layered hosts with negative-charged layers, such as montmorillonites and zirconium phosphates.[12] Macrocyclic crown ethers, the typical representative of molecular recognition and supramolecular chemistry, have sensitive and selective binding

Received: July 5, 2013
Published: December 3, 2013

   dx.doi.org/10.1021/ic4017307 | Inorg. Chem. 2013, 52, 14010–14017

properties to ions and neutral molecules, and the intercalation of crown ethers into layered compounds might impose a more rigid conformation for interlayer macrocycles, thus possibly leading to more selective ion binding. However, there has been a lack of studies focusing on this, and most of them involved layered compounds with negatively charged layers. Among these, some are through complexation interaction of electroneutral crown ethers with alkaline ions already existing in the interlayer of phyllosilicates,[13] MoS_2 or $CdPS_3$,[14] while others are via intercalation of anionic azacrowns into sulfides such as TiS_2 and TaS_2.[15] In the two above cases, the molecular cavities of crown ethers were fully occupied by metal cations,[13,14] or the molecular planes of crown ethers were parallel to the inorganic layers,[15] so the insertion of other species was blocked, and the intercalated crown ethers could not serve as secondary hosts to recognize other guests. For vertical orientation of the azacrowns in the interlayer, one excellent example is the azacrowns-zirconium phosphate composite, in which the preferred vertical crown ether favored the import of metal ions, so promoted the separation efficiency toward transition metal ions.[16] However, in the case the covalent reaction method, its use is not easy to carry out. Recently, we adopted a facile intercalation method to prepare the composites of crown ether with MgAl-LDH, in which the vertical crown ether guest acted as a second host to adsorb transition metal ions.[17] This is one novel example for crown ether compounds intercalated into positively charged layered LDH. However, up to now, there have been no reports about the intercalation of crown ether into LRH compounds. Because of the particular layer structure of the LRH, the composites may bring about novel properties. In this work, we select the NO_3^- type layered gadolinium hydroxide (NO_3-LGdH) as a precursor and prepare a composite via ion exchange of NO_3^- with an anionic carboxyethyl substituted azacrown ether (CSAE). We found the composite showed highly selective adsorption properties for transition metal and heavy metal ions.

EXPERIMENTAL SECTION

Synthesis of HCl-Form CSAE. Reagents used were of analytical grade and high purity. 4N-18-C-6 (**A**) was synthesized according to the literatures.[18] CSAE (4,7,13,16-tetracarboxyethyl-1,10-dioxa-4,7,13,16-tetraazacyclooctadecane) was synthesized from **A** according to the literature method as shown in Scheme 1.[19] Briefly, to 8 cm^3 anhydrous ethanol solution of A (0.52 g, 2 mmol), 2.7 cm^3 acrylonitrile was added in a 25 cm^3 flask. The mixture was refluxed with stirring for 24 h and then cooled. The solvent was removed by rotatory evaporation, and the resulting solid product was washed with ethanol and recrystallized with dichloromethane, then **B** was obtained. To 25 cm^3 mixed solution of HCl:H_2O (3:2), 0.40 g of **B** was added and then refluxed for 24 h. The solution was evaporated up to about 2 cm^3, and colorless crystals of HCl−form CSAE were obtained. Calcd for $C_{24}H_{44}N_4O_{10}\cdot 3HCl\cdot 3H_2O$: C, 40.48; H, 7.50; N, 7.87; Found: C, 40.36; H, 7.72; N, 7.83.

Preparation of NO_3-LGdH Precursor. The precursor NO_3-LGdH was synthesized via hydrothermal reaction of $Gd(NO_3)_3\cdot 6H_2O$ using hexamethylenetetramine (HMT) as the hydrolysis reagent. In a typical synthetic procedure, deionized water was used to dissolve 0.451 g (1 mmol) of $Gd(NO_3)_3\cdot 6H_2O$, 0.140 g (1 mmol) of HMT, and 1.105 g (13 mmol) of $NaNO_3$ to yield a 80 mL solution in a Teflon-autoclave; then the solution was sealed after purging with N_2 for 5 min and then heated at 90 °C for 12 h. The obtained product was filtered, washed, and then vacuum-dried at 40 °C for 24 h.

Intercalation of CSAE into LRH by Ion Exchange. The intercalation reactions of CSAE into NO_3-LGdH were carried out by ion exchange method at room temperature (RT, ∼20 °C) and hydrothermal reaction at 50 °C. The organic compounds were deprotonated beforehand by adding 7-fold molar excess of NaOH solid to produce the corresponding anion solutions (80 mL), with the final pH values of ∼9.30. Then the LGdH powder (0.1 g) was dispersed into the solutions. The reactions were carried out at different CSAE/LGdH weight ratios and varied temperatures of RT, 50 and 70 °C for 24 h in tapered bottles and Teflon-autoclaves, respectively. The resulting precipitates were recovered by filtration, washed with deionized water, and vacuum-dried at 40 °C for 24 h. The as-prepared composites were labeled as T*x*L-*y*, in which the number *x* is the weight ratio of CSAE/LGdH and *y* is the reacting temperature.

Adsorption Capacity for Metal Ions. A 0.05 g portion of composite T0.75L-20 was immerged with a 5 cm^3 0.01 M solution of XNO_3 (X = Li^+, Na^+, and K^+), $X(NO_3)_2$ (X = Co^{2+}, Ni^{2+}, Cu^{2+}, and Zn^{2+}), or $X(NO_3)_m$ (X = Ag^+, Pb^{2+}, Cd^{2+} or Hg^{2+}), with intermittent shaking for 3 and 7 d at RT. After the mixing, the concentrations of metal ions in the supernatant solution were determined by inductively coupled plasma (ICP). The adsorptive capacity was evaluated from the difference of metal concentrations in mother and supernatant solutions.

Distribution Coefficient (K_d) for Metal Ions. The T0.75L-20 composite (0.05 g) was immersed in 5 mL mixed solution of XNO_3 (X = Li^+, Na^+, and K^+), $X(NO_3)_2$ (X = Co^{2+}, Ni^{2+}, Cu^{2+}, and Zn^{2+}), or $X(NO_3)_m$ (X = Cu^{2+}, Ag^+, Pb^{2+}, Cd^{2+}, and Hg^{2+}) with intermittent shaking for 3 d at RT. In the above solutions, the concentration per ion is average, and the total concentration of each solution is 10 mM. For the mixed solution of Cu^{2+}, Ag^+, Pb^{2+}, Cd^{2+}, and Hg^{2+}, the concentration of each ion is about 2.5 mM. The metal ion concentrations in the supernatant solutions were determined by ICP analysis. The metal ion uptakes were calculated from the concentrations of the supernatant solution relative to initial concentrations. The distribution coefficient (K_d) values were calculated as follows

$$K_d = (V[(C_0 - C_f)/C_f])/m$$

where C_0 and C_f are respectively the initial and local concentration of M^{n+} (mM) after the contact, V is the volume (mL) of the testing solution, and m is the amount of the solid sorbent (g) used in the adsorption experiment.

Characterization Techniques. The powder X-ray diffraction (XRD) patterns were collected using a Phillips X′ pert Pro MPD diffractometer with Cu−Kα radiation, at RT, with step size of 0.0167°, scan time of 15 s per step, and 2θ ranging from 4.5 to 70°. The generator settings are 40 kV and 40 mA. Fourier transformed infrared (FT−IR) spectra of the samples were recorded on a Nicolet-380 Fourier-Transform infrared spectrometer by the KBr method. Scanning electron microscope (SEM) observations were carried out using a Hitachi S-4800 microscope at 5.0 kV. The metal ion contents were determined by inductively coupled plasma (ICP) atomic emission spectroscopy (Jarrel-ASH, ICAP-9000) after the solid products were dissolved in a 0.1 M HCl or HNO_3 solution. C, H, and N contents were determined using an Elementar vario EL elemental analyzer. The chemical formula of the products was calculated from the results of ICP and CHN analyses.

RESULTS AND DISCUSSION

Structures and Compositions of the Precursor NO_3-LGdH and Composite with CSAE. The XRD patterns of the precursor NO_3-LGdH and their ion-exchanged products with CSAE were shown in Figure 1. The NO_3-LGdH (Figure 1a) had basal reflections at 0.82 and 0.41 nm, meaning a basal spacing (d_{basal}) of 0.82 nm. The sharp and symmetric diffraction peaks suggest the product had high crystallinity with well-ordered layers. The 0.32 nm peak came from the nonbasal (220) reflection that represents the feature of the host layer,[20] so it always existed in the composites after intercalation that will be discussed later. After NO_3-LGdH reacted with different amounts of CSAE at varied temperatures, the resulting

dx.doi.org/10.1021/ic4017307 | Inorg. Chem. 2013, 52, 14010−14017

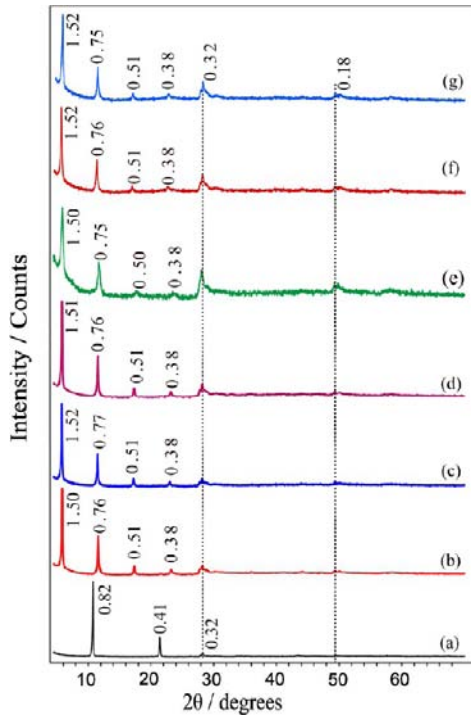

Figure 1. XRD patterns of NO_3-LGdH precursor (a) and CSAE-LGdH composite T0.5L-20 (b), T0.75L-20 (c), T1L-20 (d), T0.75L-50 (e), T1L-50 (f), and T1L-70 (g), respectively.

products displayed a series of XRD diffractions with a series of (00*l*) reflections and enlarged d_{basal} values, as shown in Figures 1b–g, demonstrating the entrance of CSAE guests into the gallery. Taking T0.5L-20 (Figure 1b) as an example, it had diffraction peaks at d = 1.50, 0.76, 0.51, 0.38, and 0.32 nm, showing a d_{basal} of 1.50 nm. The high intensities of (00*l*) reflections relative to the peaks of 2θ larger than 35° indicate the high orientation along [00*l*] directions. The much stronger intensity of the 0.32 nm peak may result from both the highly ordered host layers and the overlapped (00*l*) diffraction. The d_{basal} of the products (~ 1.5 nm) changed little when the reaction conditions varied in a certain range, though the ion-exchange degree is slightly different as shown in the composition analysis below.

Compared with the d_{basal} of ~1.6 nm in the homogeneous composite of CSAE into MgAl-LDH,[17] the present case for CSAE into LRH had a much smaller d_{basal} of ~1.5 nm. And also, the thickness of 0.65 nm for the LRH layer[21] is larger than that (0.48 nm) for the LDH layer,[22] so the interlayer CSAE in the present case corresponded to a much smaller gallery height (0.85 nm = 1.5–0.65) than that (1.1 nm = 1.6–0.48) in LDH system. The smaller gallery may be because the hard-acid rare earth ions had a stronger affinity to the hard-base oxygen atoms of the carboxyl side-arms of crown ether, based on soft–hard base-acid theory. On the other hand, the larger thickness of the LRH layer than that of the LDH layer means a larger d_{basal} of the LRH–CSAE intercalate. But quite the reverse is found; the present LRH–CSAE gave a smaller d_{basal} (~1.5 nm) than LDH–CSAE did (~1.6 nm). This further testified of the difference of LRH with LDH layers.

The compositions of the NO_3-LGdH precursor and some CSAE-LGdH composites (T0.75L-20, T1L-20, and T1L-50) were determined through ICP and CHN analyses, with chemical formula of $Gd(OH)_{2.42}(NO_3)_{0.42}(CO_3)_{0.08}\cdot 0.95H_2O$, $Gd(OH)_{2.42}(C_{24}H_{40}N_4O_{10})_{0.11}(NO_3)_{0.01}(CO_3)_{0.06}\cdot 2.7H_2O$, $Gd(OH)_{2.42}(C_{24}H_{40}N_4O_{10})_{0.12}(CO_3)_{0.05}\cdot 2.8H_2O$, and $Gd(OH)_{2.42}(C_{24}H_{40}N_4O_{10})_{0.13}(CO_3)_{0.03}\cdot 2.5H_2O$, respectively, as shown in Table 1. Compared with the precursor NO_3-LGdH, there was sharp decrease in NO_3^- content and a little decrease of CO_3^{2-} content, because of the introduction of CSAE anion. This showed most NO_3^- and some CO_3^{2-} were replaced by CSAE anions, and more CSAE added (large initial CSAE/LGdH ratios) can remove NO_3^- completely while it can much reduce CO_3^{2-} content. The presence of CO_3^{2-} rather than NO_3^- after the ion-exchange may be because CO_3^{2-} ions have a higher infinity to the LRH layer than NO_3^-, as found for the LDH system.[17,23] The information of NO_3^-/CO_3^{2-} before and after ion-exchange was also verified by IR spectra that will be described below. It is noted that though there are plenty of CO_3^{2-} ions in the interlayer, no impurity phases such as CO_3^{2-} intercalated phase can be observable, so CO_3^{2-} may coexist with CSAE ions in the 1.5 nm phase. This showed CO_3^{2-} might cointercalate with CSAE into the LRH, as we previously reported for the LDH system,[17] because of its favorable lattice stabilization enthalpy associated with the small size and high charge.[24]

IR of NO_3-LGdH Precursor and Composites. Figure 2 showed the FT-IR spectra of the as-prepared samples. In NO_3-LGdH precursor (Figure 2a), there was a strong band at 1384 cm^{-1} corresponding to the NO_3^- absorption. This band disappeared in all of the composites (Figure 2c–f), indicating the NO_3^- was exchanged completely by other ions. The band at 1353 cm^{-1} in NO_3-LGdH precursor (Figure 2a) was assigned to the absorption of CO_3^{2-}, and it still retained in all of the composites, in good agreement with the compositional analyses. In free HCl-form CSAE, the two bands at 1737 and 1412 cm^{-1} (Figure 2b) corresponding to ν_{as}(–COOH) and ν_s(–COOH) vibrations were red-shifted to 1559 and 1050 cm^{-1} in the CSAE–LGdH composites (Figures 2c–f), indicating that carboxyl groups were in a deprotonated form ($-COO^-$) after the intercalation. In addition, the band at 1132 cm^{-1} assigned to the C–O–C ring vibrations in CSAE (Figure 2b) was shifted to 1115 cm^{-1}, which showed there existed strong H-bonding interaction between the oxygen atoms of the crown ether ring and hydroxyl groups of the LRH layers and/or interlayer water molecules. The bands observed around 2900 cm^{-1} were assigned to the stretching vibrations of $-CH_2$

Table 1. Chemical Composition for the Precursor and CSAE/LRH Composites

samples	chemical formula $L = C_{24}H_{40}N_4O_{10}^{4-}$	content, found (calcd)/%			
		C	H	N	Gd
NO_3-LGdH	$Gd(OH)_{2.42}(NO_3)_{0.42}(CO_3)_{0.08}\cdot 0.95H_2O$	0.42 (0.39)	1.92 (1.77)	2.40 (2.39)	64.04 (63.82)
T0.75L-20	$Gd(OH)_{2.42}(L)_{0.11}(NO_3)_{0.01}(CO_3)_{0.06}\cdot 2.7H_2O$	11.07 (10.43)	3.61 (3.95)	1.96 (2.02)	50.19 (50.48)
T1L-20	$Gd(OH)_{2.42}(L)_{0.12}(CO_3)_{0.05}\cdot 2.8H_2O$	11.45 (11.09)	3.88 (4.07)	1.94 (2.12)	49.66 (49.55)
T1L-50	$Gd(OH)_{2.42}(L)_{0.13}(CO_3)_{0.03}\cdot 2.5H_2O$	12.10 (12.01)	3.74 (4.00)	2.08 (2.31)	50.07 (49.90)

dx.doi.org/10.1021/ic4017307 | Inorg. Chem. 2013, 52, 14010–14017

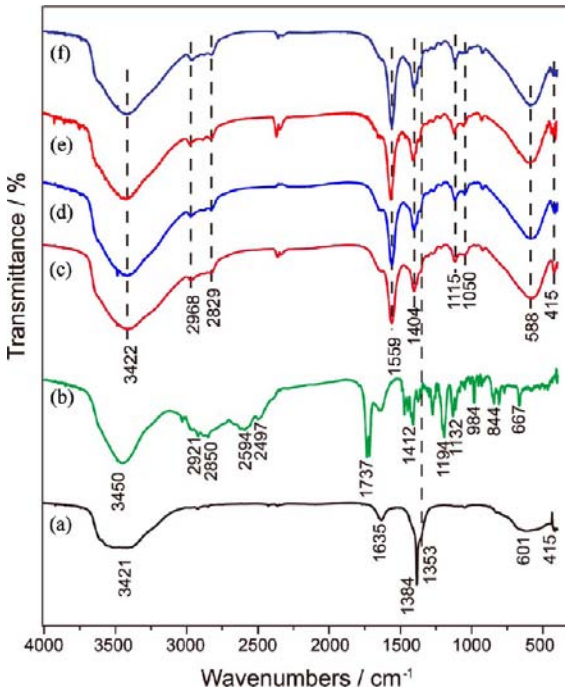

Figure 2. IR spectra of NO_3-LGdH (a), CSAE (b), CSAE-LGdH composite T0.5L-20 (c), T0.75L-20 (d), T1L-20 (e), and T1L-70 (f), respectively.

groups of CSAE, and those at 601/588 and 415 cm^{-1} belonged to the ν(M-O) and δ(O-M-O) vibrations, respectively. The red-shift of ν(M-O) vibration from 601 cm^{-1} in NO_3-LGdH precursor to 588 cm^{-1} after intercalation may also result from H-bonding interaction of crown ether anions with the layer hydroxyl groups. All of these results exhibited the introduction of CSAE and its interaction with the LRH layer.

Morphology of NO_3-LGdH Precursor and Composites. SEM observations (Figure 3) revealed the microstructure and morphology of the as-prepared products. The samples were dispersed in ethanol and then subjected to SEM observations. As shown in Figures 3a,a′, NO_3-LGdH precursor revealed well-shaped columnar aggregates, and some well developed elongated hexagonal plates with edge lengths of about ~8 × 20 μm^2 were also observable, all of which are consistent with the characteristics of a layered compound. The CSAE−LGdH composites with a similar morphology to that mentioned above were also observed. They grew into columnar aggregates like dominoes, as shown in Figures 3b−d′. The hydrothermal reaction caused the roughness of the sample surface with some irregular fragments appearing on the facet, although the basic layered skeleton was retained (Figures 3e,e′,f,f′).

Adsorptive Properties toward Heavy Metal Ions of the Composite. The adsorptive capacities of the composite T0.75L-20 toward metal ions were measured by a batch method. The adsorptive data were listed in Tables 2, 3, and 4. For transition metal ions, the composite exhibited obvious adsorptive capacities, with the orders of adsorptive capacity of $Cu^{2+} \gg Zn^{2+} \sim Ni^{2+} \sim Co^{2+}$, and when putting these ions together, Cu^{2+} revealed a notable high adsorptive selectivity with respect to others. The higher removal ability for Cu^{2+} may correspond to its special stabilization energy resulting from the Jahn−Teller effect. For heavy metal ions, the composite also revealed obvious adsorptive capacities, and showed high selectivity for Ag^+ and Hg^{2+}. For alkali metal ions, the

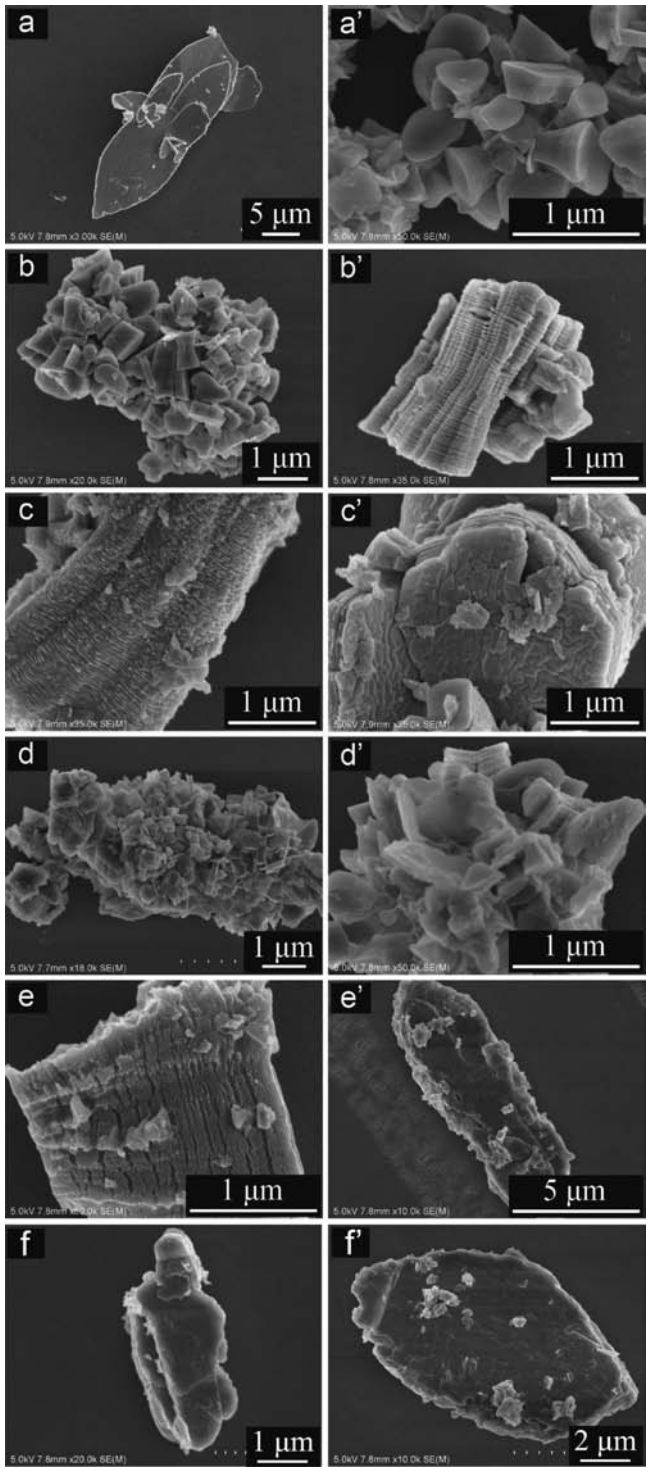

Figure 3. SEM images of NO_3-LGdH (a,a′), CSAE-LGdH composite T0.5L-20 (b, b′), T0.75L-20 (c, c′), T1L-20 (d, d′), T1L-50 (e, e′), and T1L-70 (f, f′), respectively.

composite has little adsorptive capacity and selectivity. The better adsorption for transition and heavy metal ions than for alkali metal ions is in good agreement with the soft−hard base-acid theory. The CSAE anions with four soft-base nitrogen atoms have higher affinity to soft-acid transition or heavy metal ions rather than hard-acid alkali metals. Additionally, we can see the adsorption of ions impacted each other, because the ion uptakes changed much in mixed solutions than in single ones.

dx.doi.org/10.1021/ic4017307 | Inorg. Chem. 2013, 52, 14010−14017

Table 2. Adsorptive Capacity toward Metal Ions of the Composite T0.75L-20[a]

	initial solution		after 3d adsorption		adsorptive capacity	
single ions	C_0 (mM)	pH	C_f (mM)	pH	ion uptakes (mg·g^{-1})	M^{n+} removal (%)
Li^+	10.49	6.10	9.12	7.47	0.01	13.1
Na^+	9.74	5.72	9.57	7.45	0.44	1.7
K^+	9.07	5.40	9.69	6.81		
Co^{2+}	11.27	5.90	8.48	7.25	16.50	24.8
Ni^{2+}	10.87	5.79	8.70	7.10	12.91	20.0
Cu^{2+}	10.56	4.94	3.09	6.71	47.66	70.7
Zn^{2+}	10.14	5.74	7.35	6.93	18.31	27.5
Ag^+	9.96	5.60	6.43	6.32	37.75	35.5
Pb^{2+}	10.25	4.85	6.28	6.76	82.88	38.7
Cd^{2+}	10.88	5.80	6.92	6.80	44.96	36.4
Hg^{2+}	8.53	2.65	4.84	7.01	74.18	43.2

[a]0.05 g solid, 5 cm^3 solution of $X(NO_3)_m$ with a 10 mM concentration for each ion.

Table 3. Adsorptive Selectivity (Distribution Coefficient, K_d) toward Metal Ions by T0.75L-20[a]

	initial solution	after 3d adsorption		
mixed ions	C_0 (mM)	C_f (mM)	M^{n+} removal (%)	K_d (mL/g)
Li^+	3.46	3.44	0.6	0.6
Na^+	3.37	3.18	5.6	6.0
K^+	3.24	3.23	0.3	0.3
		pH 5.56 → 7.36		
Co^{2+}	2.81	2.61	7.1	8
Ni^{2+}	2.71	1.96	27.7	38
Cu^{2+}	2.79	1.29	53.8	116
Zn^{2+}	2.77	1.92	30.7	44
		pH 5.25→ 6.98		
Ag^+	2.62	0.15	94.1	1610
Pb^{2+}	2.61	2.12	18.6	23
Cd^{2+}	2.62	2.67	–	–
Hg^{2+}	4.24	1.30	69.3	225
		pH 2.85→ 6.72		

[a]0.05 g solid, 5 cm^3 mixed solution with a total concentration of 10 mM XNO_3 (X = Li^+, Na^+, and K^+), $X(NO_3)_2$ (X = Co^{2+}, Ni^{2+}, Cu^{2+}, and Zn^{2+}), or $X(NO_3)_m$ (X = Ag^+, Hg^{2+}, Pb^{2+}, and Cd^{2+}), respectively.

Table 4. Adsorptive Results of T0.75L-20 toward Cu^{2+}, Ag^+, Pb^{2+}, Cd^{2+} and Hg^{2+} Ions[a]

	initial solution	after 3d adsorption		
mixed ions	C_0 (mM)	C_f (mM)	M^{n+} removal (%)	K_d (mL/g)
Cu^{2+}	2.59	1.60	37.0	62
Ag^+	2.65	0.03	99.0	9712
Pb^{2+}	2.67	2.22	17.0	20
Cd^{2+}	2.50	2.33	2.7	3
Hg^{2+}	2.95	1.23	58.1	139

[a]0.05 g solid, 5 cm^3 mixed solution of Cu^{2+}, Ag^+, Pb^{2+}, Cd^{2+}, and Hg^{2+} with a ~2.5 mM concentration per ion.

For example, the adsorptive capacity are very close for heavy metal ions Ag^+, Hg^{2+}, Pb^{2+}, and Cd^{2+}, but when putting these ions together, the K_d values had an obvious orders of $Ag^+ \gg Hg^{2+} \gg Pb^{2+} > Cd^{2+}$, showing a high selectivity toward Ag^+ and Hg^{2+}. In addition, when putting the five ions of Cu^{2+}, Ag^+, Hg^{2+}, Pb^{2+}, and Cd^{2+} together, the adsorptive experiments gave a selectivity order of $Ag^+ \gg Hg^{2+} > Pb^{2+} > Cu^{2+} > Cd^{2+}$. This indicates that the heavy metal ions as Ag^+ and Hg^{2+} have obvious adsorptive selectivity over Pb^{2+} and Cd^{2+}, and Cu^{2+} has also the relatively high selectivity but not as high as Ag^+ and Hg^{2+}. In any case, Cd^{2+} has nearly no adsorption under the mixed state using this kind of material, showing a bad selectivity. The phenomenon reveals that the adsorption of preferential ions holds back the adsorption of other ions. In addition, we found that the adsorptive capacities of the metal ions during 7 and 3 d are nearly the same, showing that 3 d time is enough for the accomplishment of the adsorption experiments.

The metal ion adsorption was accompanied by the adsorption of NO_3^- ions, which was shown by the FT-IR spectra (Figures 4, 5) of the solids after metal adsorption. The

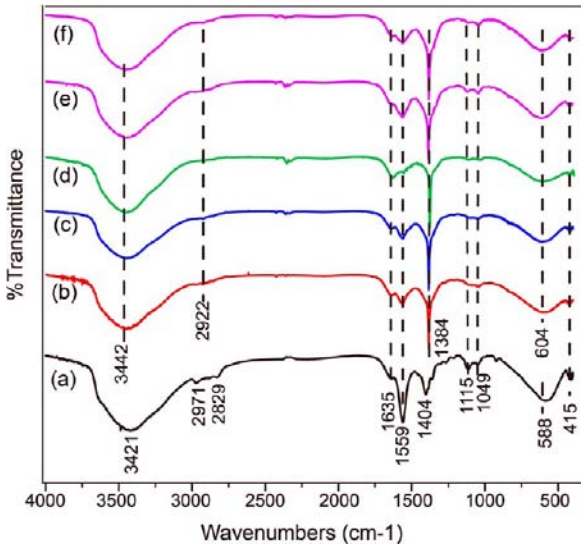

Figure 4. IR spectra of the solids of T0.75L-20 (a) and after it adsorbed Co^{2+} (b), Ni^{2+} (c), Cu^{2+} (d), Zn^{2+} (e), and their mixed solution (f), respectively.

strong $\nu_{as}(NO_3^-)$ vibration at 1384 cm^{-1} indicated the existence of NO_3^-. The relatively weak NO_3^- band for the Ag^+ adsorbed sample (Figure 5b) may be due to the +1 charge of Ag^+ resulting in less corresponding accompanied NO_3^-. This revealed that the adsorption of metal ions progresses by insertion as a neutral salt by virtue of the complexation interaction with the crown ether, rather than by conventional cation exchange reaction. This result also showed that the

dx.doi.org/10.1021/ic4017307 | Inorg. Chem. 2013, 52, 14010−14017

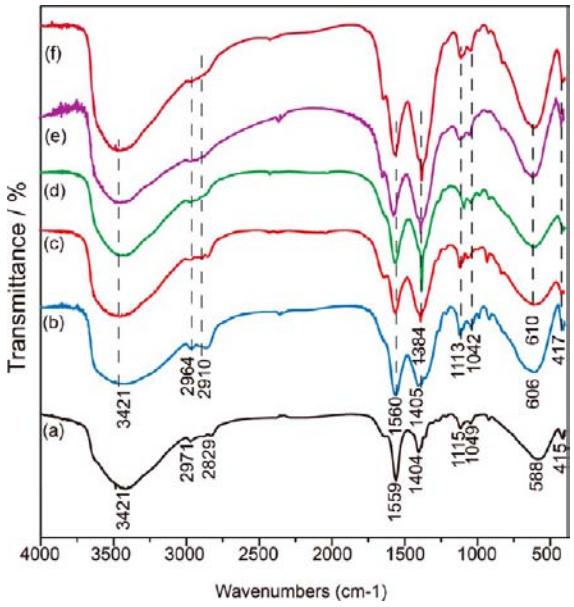

Figure 5. IR spectra of solids after T0.75L-20 (a) adsorbed Ag^+ (b), Pb^{2+} (c), Cd^{2+} (d), Hg^{2+} (e), and the mixed solution (f), respectively.

intercalated CSAE ions acted as a second host to introduce guest salts. Another important point in the IR spectra is the shift of the ν(M-O) vibrations from 588 to 604/606 cm^{-1} after adsorption. This may have further verified the coordination interaction of the adsorbed metal ions with the crown ether anions, which reduced the H-bonding of the crown ether with the layer hydroxyl groups, and thus increased the combination ability of the layer hydroxyl groups with the layer metal ions, resulting in the blue-shift of ν(M-O) vibrations.

In the metal adsorption process, we can find a phenomenon that the pH values of the solutions increase generally after adsorption. We think this may be also evidence of the removal of acidic metal nitrate salts. From the pH values of initial salt solutions, we know the low pH resulted from the hydrolyzation of the salts, with the exclusion of the much lower pH of Hg^{2+} solution because of the usage of acid to dissolve $Hg(NO_3)_2$. When the composite solid contacted with the solution, the metal nitrate salts were removed quickly so as to reduce the possibility of their hydrolyzation, thus increasing the pH values of the solution. Additionally, partial decomposition of the layer hydroxides and their combination to the protons in solution may also lead to the pH increase. So the increase of pH values after adsorption may be a collective effect of the removal of acidic metal salts and partial dissolution of the LRH solid.

Figures 6−8 are the XRD patterns of the solids after the adsorption. Based on them, we can find that the d_{basal} of the solids after the adsorption has changed little for alkali metal ions, while it decreased for transition metal ions (except Co^{2+} and Ni^{2+}) and Pb^{2+}, Hg^{2+}, but on the contrary increased for Ag^+ and Cd^{2+}. The results may be explained by the different ion radii of the adsorbed ions and their varied coordination motifs. The metal ions can coordinate not only with the nitrogen and oxygen atoms of the crown ring but also with the oxygen atoms of carboxyl side-arms, varying along with the kinds of metal ions. It is noted that Cu^{2+} ions have particular and flexible coordinated modes such as four-, five-, and six-coordination geometries due to the Jahn−Teller effect. As shown in the crystal structure (Supporting Information, Figure S1) of Cu^{2+} with free CSAE anion,[19] we see a binuclear Cu^{2+} complex was

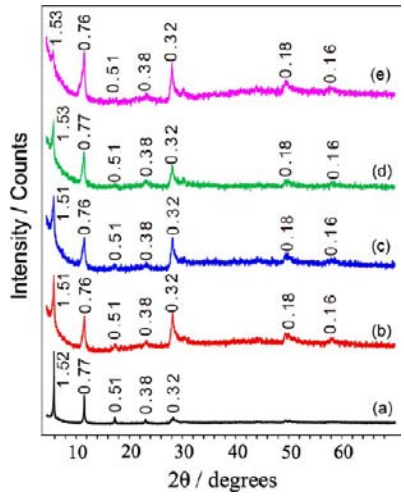

Figure 6. XRD patterns of the solids T0.75L-20 (a) and those after it adsorbed Li^+ (b), Na^+ (c), K^+ (d), and their mixed solution (e), respectively.

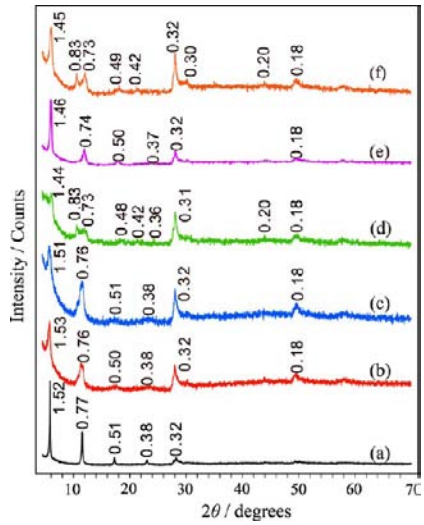

Figure 7. XRD patterns of the solid of T0.75L-20 (a) and those after it adsorbed Co^{2+} (b), Ni^{2+} (c), Cu^{2+} (d), Zn^{2+} (e), and their mixed solution (f), respectively.

formed, in which one Cu^{2+} is coordinated to two N atoms of the ring, two O atoms of two carboxylic groups, and one O atom of one water molecule, forming a five-coordinating geometry; at the same time, another Cu^{2+} is coordinated to the other two N atoms of the crown ring, two O atoms of the other two carboxylic groups and another one water O atom, showing the same coordinating environments. Additionally, the two Cu^{2+} ions distributed on the two sides (left and right) of the crown ether molecule and made the ring twist and so led to a decreased d_{basal}, compared with the extended fashion with two of the four negative-charged carboxylic arms combined with one layer and the other two attached to another layer through electrostatic interaction. Certainly, in the case of decreased d_{basal}, the coordination may be also a mononuclear mode, in which the crown ether ring is much distorted and metal ions coordinate mainly with the nitrogen and oxygen atoms of the crown ring.

In the case of increased d_{basal}, taking Ag^+ as an example, the coordination mode may be multinuclear, for which metal ions

dx.doi.org/10.1021/ic4017307 | Inorg. Chem. 2013, 52, 14010−14017

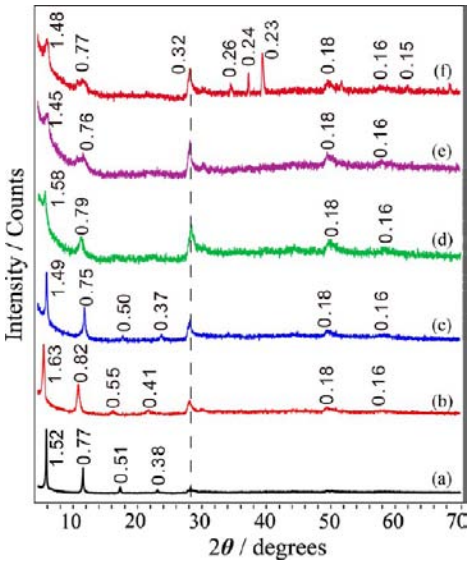

Figure 8. XRD patterns of the solid T0.75L-20 (a) and those after it adsorbed Ag^+ (b), Pb^{2+} (c), Cd^{2+} (d), Hg^{2+} (e), and their mixed solution (f), respectively.

can coordinate with both the N/O atoms of crown ether ring and O atoms of the carboxyl side-arms of CSAE, and also, the very large ion radii of Ag^+ may contribute to the increase of d_{basal}. Additionally, from the XRD patterns of the samples after adsorption experiments for 7 d, the LRH layer retained well, which showed the composite material is stable in the operational salt solutions, revealing its practical utility.

From the above results, we can see that this kind of nanocomposites with a second host in the interlayer are promising materials because specific properties can be expected by the synergy of the steric effect of the parent host and the supermolecular recognition of the intercalated secondary host.

CONCLUSIONS

One azacrown ether carboxylic acid derivative (abbr. CSAE) was successfully intercalated into a well-crystallized NO_3-LGdH. Larger initial weight ratio of CSAE/LGdH gave a higher degree of ion exchange, accompanying increased CSAE content and decreased CO_3^{2-} content. The intercalated CSAE ions in the composites kept an obvious adsorption to transition and heavy metal ions, especially with high selectivity to Cu^{2+}, Ag^+, and Hg^{2+}, but with a poor adsorption to alkali metal ions. This is in keeping with the soft–hard base-acid theory: CSAE anions with four soft-base nitrogen atoms have higher affinity to soft-acid transition metals and heavy metals rather than hard-acid alkali metals. The adsorption for metal ions was accompanied by intercalation of nitrate anions. The LRH layers of the composites remained invariable after adsorption, showing a strong stability. The d_{basal} of the solid samples changed differently after adsorbing varied metal ions, which may be related to the different coordination atoms and coordination motifs. Mononuclear coordination with nitrogen and/or oxygen atoms of the crown ring may lead to the twist or compactness of the crown ring and thus the decreased d_{basal}, while multinuclear coordination with not only the crown ring but also oxygen atoms of the carboxyl side-arms of CSAE might cause the expansion of the crown ring and then an increased d_{basal}. The composite with a double-host structure may be promising as a new kind of separation material because of the cooperative host–guest characteristics of the parent and the second hosts.

ASSOCIATED CONTENT

Supporting Information

The synthesis route of HCl-form CSAE and the crystal structure of the free CSAE anion with Cu^{2+}. This material is available free of charge via the Internet at http://pubs.acs.org.

AUTHOR INFORMATION

Corresponding Author

*E-mail: mashulan@bnu.edu.cn. Fax: +86-10-5880-2075. Phone: +86-10-5880-7524.

Notes

The authors declare no competing financial interest.

ACKNOWLEDGMENTS

This work is supported by the National Science Foundations of China 21271028, 51272030, 21271001, and Beijing Municipal Natural Science Foundation 2112022.

REFERENCES

(1) (a) Lopes, W. A.; Jaeger, H. M. *Nature* **2001**, *414*, 735. (b) Ma, R.; Sasaki, T. *Adv. Mater.* **2010**, *22*, 5082. (c) Coronado, E.; Marti-Gastaldo, C.; Navarro-Moratalla, E.; Ribera, A.; Blundell, S. J.; Baker, P. J. *Nat. Chem.* **2010**, *2*, 1031. (d) Zhao, J.-W.; Kong, X.-G.; Shi, W.-Y.; Shao, M.-F.; Han, J.-B.; Wei, M.; Evans, D. G.; Duan, X. *J. Mater. Chem.* **2011**, *21*, 13926. (e) Han, J. B.; Dou, Y. B.; Yan, D. P.; Ma, J.; Wei, M.; Evans, D. G.; Duan, X. *Chem. Commun.* **2011**, *47*, 5274. (f) Dou, Y. B.; Pan, T.; Zhou, A.; Xu, S. M.; Liu, X. X.; Han, J. B.; Wei, M.; David, D. G.; Duan, X. *Chem. Commun.* **2013**, *49*, 8462–8464.

(2) (a) Ogawa, M.; Kuroda, K. *Chem. Rev.* **1995**, *95*, 399. (b) Khan, A. I.; O'Hare, D. *J. Mater. Chem.* **2002**, *12*, 3191. (c) Evans, D. G.; Duan, X. *Chem. Commun.* **2006**, 485. (d) Geng, F.; Ma, R.; Sasaki, T. *Acc. Chem. Res.* **2010**, *43*, 1177. (e) Manos, M. J.; Kanatzidis, M. G. *J. Am. Chem. Soc.* **2012**, *134*, 16441. (f) Lee, B.-I.; Lee, E.-s.; Byeon, S.-H. *Adv. Funct. Mater.* **2012**, *22*, 3562. (g) Nicolosi, V.; Chhowalla, M.; Kanatzidis, M. G.; Strano, M. S.; Coleman, J. N. *Science* **2013**, *340*, 1226419.

(3) Gandara, F.; Perles, J.; Snejko, N.; Iglesias, M.; Gomez-Lor, B.; Gutierrez-Puebla, E. M.; Monge, A. *Angew. Chem., Int. Ed.* **2006**, *45*, 7998.

(4) (a) Lee, B.-I.; Lee, K. S.; Lee, J. H.; Lee, I. S.; Byeon, S.-H. *Dalton Trans.* **2009**, 2490. (b) Gu, Z.; Thomas, A. C.; Xu, Z. P.; Campbell, J. H.; Lu, G. Q. *Chem. Mater.* **2008**, *20*, 3715. (c) Yoon, Y.; Lee, B. I.; Lee, K. S.; Im, G. H.; Byeon, S. H.; Lee, J. H.; Lee, I. U. *Adv. Funct. Mater.* **2009**, *19*, 3375.

(5) (a) Hu, L. F.; Ma, R. Z.; Ozawa, T. C.; Sasaki, T. *Angew. Chem., Int. Ed.* **2009**, *48*, 3846. (b) Hu, L. F.; Ma, R. Z.; Ozawa, T. C.; Geng, F. X.; Iyi, N.; Sasaki, T. *Chem. Commun.* **2008**, *40*, 4897. (c) Hu, L. F.; Ma, R. Z.; Ozawa, T. C.; Sasaki, T. *Inorg. Chem.* **2010**, *49*, 2960.

(6) Gándara, F.; Puebla, E. G.; Iglesias, M.; Proserpio, D. M.; Snejko, N.; Monge, M. Á. *Chem. Mater.* **2009**, *21*, 655.

(7) (a) Lee, K.-H.; Byeon, S. -H. *Eur. J. Inorg. Chem.* **2009**, 929. (b) Geng, F. X.; Xin, H.; Matsushita, Y.; Ma, R.; Tanaka, M.; Izumi, F.; Iyi, N.; Sasaki, T. *Chem.—Eur. J.* **2008**, *14*, 9255. (c) Geng, F. X.; Matsushita, Y.; Ma, R.; Xin, H.; Tanaka, M.; Izumi, F.; Iyi, N.; Sasaki, T. *J. Am. Chem. Soc.* **2008**, *130*, 16344. (d) Geng, F.; Matsushita, Y.; Ma, R.; Xin, H.; Tanaka, M.; Iyi, N.; Sasaki, T. *Inorg. Chem.* **2009**, *48*, 6724. (e) Liang, J. B.; Ma, R.; Geng, F. X.; Ebina, Y.; Sasaki, T. *Chem. Mater.* **2010**, *22*, 6001. (f) Wu, X. L.; Li, J. G.; Li, J. K.; Zhu, Q.; Li, X. D.; Sun, X. D.; Sakka, Y. *Sci. Technol. Adv. Mater.* **2013**, *14*, 015006.

(8) (a) Wang, P. P.; Bai, B.; Hu, S.; Zhuang, J.; Wang, X. *J. Am. Chem. Soc.* **2009**, *131*, 16953. (b) Wang, P. P.; Bai, B.; Huang, L. J.; Hu, S.; Zhuang, J.; Wang, X. *Nanoscale* **2011**, *3*, 2529. (c) Zhao, Y. S.; Li, J. G.; Guo, M. X.; Yang, X. J. *J. Mater. Chem. C* **2013**, *1*, 3584.

(9) (a) Chu, N. K.; Sun, Y. H.; Zhao, Y. S.; Li, X. X.; Sun, G. B.; Ma, S. L.; Yang, X. J. *Dalton Trans.* **2012**, *41*, 7409. (b) Gu, Q. Y.; Sun, Y. H.; Chu, N. K.; Ma, S. L.; Jia, Z. Q.; Yang, X. J. *Eur. J. Inorg. Chem.* **2012**, 4407. (c) Sun, Y. H.; Chu, N. K.; Gu, Q. Y.; Pan, G. H.; Sun, G. B.; Ma, S. L.; Yang, X. J. *Eur. J. Inorg. Chem.* **2013**, 32. (d) Sun, Y. H.; Pan, G. H.; Gu, Q. Y.; Li, X. X.; Sun, G. B.; Ma, S. L.; Yang, X. J. *Mater. Res. Bull.* **2013**, *48*, 4460.

(10) (a) Izatt, R. M.; Christensen, J. J. *Synthesis of Macrocycles: The Design of Selective Complexing Agents*; Wiley-Interscience: New York, 1987. (b) Vögtle, F.; Weber, E. *Host Guest Complex Chemistry Macrocycles*; Springer-Verlag: Berlin, Germany, 1985.

(11) (a) Lehn, J. M. *Science* **1985**, *227*, 849. (b) Lindoy, L. F. *The chemistry of macrocyclic ligand complexes*; Cambridge University Press, Cambridge, U.K., 1989. (c) Zhao, H.; Vance, G. F. *J. Chem. Soc., Dalton Trans.* **1997**, 1961.

(12) (a) Kijima, T.; Tanaka, J.; Goto, M.; Matsui, Y. *Nature* **1984**, *310*, 45. (b) Kijima, T.; Kobayashi, M.; Matsui, Y. *J. Inclusion Phenom.* **1985**, *2*, 807. (c) Kijima, T.; Matsui, Y. *Nature* **1986**, *322*, 533.

(13) (a) Herber, R. H.; Cassell, R. A. *J. Chem. Phys.* **1981**, *75*, 4669. (b) Herber, R. H.; Cassell, R. A. *Inorg. Chem.* **1982**, *21*, 3713.

(14) (a) Lara, N.; Ruiz-Hitzky, E. *J. Braz. Chem. Soc.* **1996**, *7*, 193. (b) Glueck, D. S.; Brough, A. R.; Mountford, P.; Green, M. L. H. *Inorg. Chem.* **1993**, *32*, 1893.

(15) Villanueva, A.; Ruiz-Hitzky, E. *J. Mater. Chem.* **2004**, *14*, 824.

(16) (a) Alberti, G.; Boccali, L.; Dionigi, C.; Kalchenko, V. I.; Vivani, R.; Atamas, L. I. *Supramol. Chem.* **1996**, *7*, 129. (b) Zhang, B. L.; Clearfield, A. *J. Am. Chem. Soc.* **1997**, *119*, 2751.

(17) Ma, S. L.; Fan, C. H.; Du, L.; Huang, G. L.; Yang, X. J.; Tang, W. P. Y.; Makita, K. O. *Chem. Mater.* **2009**, *21*, 3602.

(18) (a) Biernat, J. F.; Luboch, E. *Tetrahedron* **1984**, *40*, 1927. (b) Ma, S. L.; Zhu, W. X.; Gao, S.; Guo, Q. L.; Xu, M. Q. *Eur. J. Inorg. Chem.* **2004**, 1311.

(19) Xu, M. Q. Master Dissertation, Beijing Normal University, Beijing, China, 2004.

(20) Wang, L.; Yan, D. P.; Qin, S. H.; Li, S. D.; Lu, J. D.; Evans, G.; Duan, X. *Dalton Trans.* **2011**, *40*, 11781.

(21) Wang, L. Master Dissertation, Beijing University of Chemical Technology, Beijing, China, 2010.

(22) Miyata, S. *Clays Clay Miner.* **1975**, *23*, 369.

(23) Miyata, S. *Clays Clay Miner.* **1983**, *31*, 305.

(24) Oriakhi, C. O.; Farr, I. V.; Lerner, M. M. *J. Mater. Chem.* **1996**, *6*, 103.